

A Simplified Method Based on Magnetic Measurement for Determination of Iron-Core Tokamak Plasma Current Center

Zhe Xing¹ · Bingjia Xiao^{1,2} · Jinping Qian¹

Published online: 1 July 2015

© Springer Science+Business Media New York 2015

Abstract For the safe and efficient discharge operation, it is essential to real-time determine the plasma current center and guide the parameters modification in the vertical field coil current feedback control system. In this paper, we analyze the limitation of the method of measuring the plasma displacement by using single-turn loops, which was used in the vertical field coil current feedback control system on iron-core tokamak HT-7. In addition, we introduce a new method to estimate the plasma current center using the external magnetic measurements on iron-core tokamak. This method has been validated by several HT-7 discharges. The simulation and discussion of measured values by this method is presented.

Keywords Iron-core tokamak · Plasma current center · Magnetic measurement

Introduction

In the tokamak, the magnetic pressure of toroidal magnetic field acts together with the internal pressure (kinetic pressure) which is created by the hot gas to expand the plasma along the major radius [1]. In addition, the magnetic pressure of poloidal magnetic field further strengthens the outward power [1]. There is only the magnetic tension of toroidal magnetic field used as a reverse force to balance the outward force along the

major radius, which is often not enough. In order to maintain equilibrium along the major radius, an external vertical magnetic field is necessary and available to present an inward force [2, 3]. The external vertical field is operated by the feedback control system, which bases on the estimation of the position of plasma current center [4]. Therefore, the determination of the plasma current center is very important for tokamak discharge experiments.

The plasma current center cannot be measured directly. We could only evaluate the position by external magnetic measurements. Firstly, we introduce and analyze the previous method on HT-7, which measure the plasma displacement by the single-turn flux loops [5]. This displacement was used in the vertical field feedback control replacing the plasma current center. Secondly, we used a new method, which has been successfully applied on EAST [4], to evaluate the plasma current center from magnetic diagnostic signals. At last, we analyzed the calculation results and estimated the measured plasma displacement value in HT-7 experiments.

Measurement of the Plasma Displacement by Single-Turn Flux Loops

In the tokamak, we can use a single-turn flux loop that wrap toroidally around the torus to measure the poloidal flux Ψ . In the large aspect-ratio approximation, the flux is written in the form [6]

$$\Psi(\rho_M, \omega_M) = \frac{\mu_0 I_p R_p}{2\pi} \left(\ln \frac{8R_p}{\rho_M} - 2 \right) - \frac{\mu_0 I_p}{4\pi} \left(\ln \frac{\rho_M}{a_p} + \left(A + \frac{1}{2} \right) \left(1 - \frac{a_p^2}{\rho_M^2} \right) \right) \rho_M \cos \omega_M \quad (1)$$

✉ Zhe Xing
xzpb@ipp.ac.cn

¹ Institute of Plasma Physics, Chinese Academy of Sciences, PO Box 1126, Hefei 230031, Anhui, China

² School of Nuclear Science and Technology, University of Science and Technology of China, Hefei 230027, Anhui, China

Here, (ρ_M, ω_M) is the coordinates of measurement point, $A = \beta_\theta + \frac{\xi}{2} - 1$ and (R_p, a_p) are the plasma major radius and minor radius. Note that $R_p = R_0 - \Delta x$ and $a_p = a_0 - \sqrt{\Delta x^2 + \Delta y^2}$, here (R_0, a_0) are the tokamak major radius and the minor radius. To be convenient, based on the assumption that $\Delta r \ll a_p < a_0 \ll R_0$, the formula (1) can be expanded to the harmonic form [5] around (R_0, a_0) :

$$\Psi(\rho_0, \omega) = \Psi_0 + \sum_{m=1}^{\infty} \Psi_X^m \cos m\omega + \sum_{n=1}^{\infty} \Psi_Y^n \sin n\omega \quad (2)$$

Here, (ρ_0, ω) is the coordinates of measurement point in the quasicylindrical coordinates. Then, we can derive that:

$$\begin{cases} \Psi(\rho_0, \omega) + \Psi(\rho_0, -\omega) = 2\Psi_0 + 2 \sum_{m=1}^{\infty} \Psi_X^m \cos m\omega \\ \Psi(\rho_0, \omega) - \Psi(\rho_0, -\omega) = 2 \sum_{n=1}^{\infty} \Psi_Y^n \sin n\omega \end{cases} \quad (3)$$

Neglecting second and higher order of $\Delta x, \Delta y, \Delta r$, the plasma displacement can be calculated by the equations below [4, 5]:

$$\begin{cases} \left[\Psi\left(\rho_0, \frac{\pi}{4}\right) + \Psi\left(\rho_0, -\frac{\pi}{4}\right) - \Psi\left(\rho_0, \frac{3\pi}{4}\right) - \Psi\left(\rho_0, -\frac{3\pi}{4}\right) \right] / \frac{\sqrt{2}\mu_0 I_p R_0}{\pi\rho_0} = \Delta x - \frac{\rho_0^2}{2R_0} \ln \frac{\rho_0}{a_0} - \frac{\rho_0^2 - a_0^2}{2R_0} \left(A + \frac{1}{2} \right) \\ \left[\Psi\left(\rho_0, \frac{\pi}{4}\right) - \Psi\left(\rho_0, -\frac{\pi}{4}\right) + \Psi\left(\rho_0, \frac{3\pi}{4}\right) - \Psi\left(\rho_0, -\frac{3\pi}{4}\right) \right] / \frac{\sqrt{2}\mu_0 I_p R_0}{\pi\rho_0} = -\Delta y \end{cases} \quad (4)$$

Here, ρ_0 is the radius of the single-turn loop. Based on the formulas (4), we can use four single-turn loops, which are distributed equally in the toroidal direction, to measure $(\Delta x, \Delta y)$. Here $(\Delta x, \Delta y)$ presents the plasma displacement relative to the tokamak center (R_0, a_0) . What calls for special attention is that the formula (2–4) can be applicable only if $\Delta r \ll a_p < a_0 \ll R_0$.

As shown in formula (4), the horizontal displacement Δx cannot be determined directly by using the four single-turn loops. There is an offset value $\frac{\rho_0^2}{2R_0} \ln \frac{\rho_0}{a_0} + \frac{\rho_0^2 - a_0^2}{2R_0} \left(A + \frac{1}{2} \right)$, which is known as Shafranov shift [1], between the measured value and Δx . The Shafranov shift is not a constant and hard to be measured directly during discharge, especially in the plasma breakdown phase. On the other hand, based on the calculation by formula (4), the vertical displacement Δy can be directly measured by using the four single-turn loops. In the results section below, we will give the simulation results about this method and evaluate its application.

Estimation of the Position of Plasma Current Center by Magnetic Measurement

As mentioned above, we could evaluate the position of plasma current center from magnetic diagnostic signals in EAST [4]. In the following, we will introduce the proven method of estimating the plasma current center by using magnetic measurement.

The Plasma Current Center Prediction

As we known, the total poloidal magnetic field measured by the poloidal magnetic probe array on HT-7 is induced by the toroidal current that flows inside the plasma and external poloidal field coils.

$$\begin{pmatrix} B_t \\ B_n \end{pmatrix} = \begin{pmatrix} G_{tc} \cdot I_c + G_{tp} \cdot I_p \\ G_{nc} \cdot I_c + G_{np} \cdot I_p \end{pmatrix} \quad (5)$$

Here, B_t and B_n are the magnetic field in the tangential and the radial direction, $(G_{tc}, G_{tp}, G_{nc}, G_{np})$ are the response matrices which are used to calculate the magnetic field by

multiplying current, the subscript t, n refer to the tangential and the radial direction respectively and c, p refer to external poloidal field coils and plasma respectively, I_c is the external field coils current vector, and I_p is the plasma current vector on the grids inside the vacuum vessel.

On HT-7, the poloidal magnetic field is measured by magnetic probe array. The array consists of 12 magnetic probes distributed equally in the circle poloidal direction [7]. Each probe can measure the magnetic field in the tangential direction (B_t) and the radial direction (B_n). The currents of poloidal field coils, including ohmic field coils, vertical field coils and horizontal field coils, are measured by separate Rogowski coils outside the vacuum vessel [7]. The formula (5) can be turned to formula (6).

$$I_p = \begin{pmatrix} G_{tp} \\ G_{np} \end{pmatrix}^{-1} \cdot M \cdot \begin{pmatrix} -I_c \\ B_t \\ B_n \end{pmatrix} \quad (6)$$

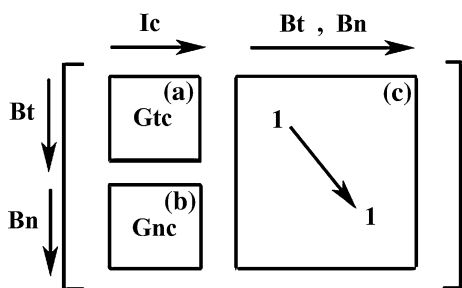


Fig. 1 A schematic flow of the matrix M

The diagram in Fig. 1 shows the schematic flow of the matrix M. Blocks (a) and (b) in the matrix M contain the response matrices G_{tc} , G_{nc} . Block (c) is a unit matrix, and its order is the amount of the magnetic measurement elements used for the prediction of plasma current center. On HT-7, we divide the vacuum vessel into 33×33 segments. According to the typical plasma current distribution, we calculate the plasma filament current in the segments. Each element of the plasma current vector I_p corresponds to the plasma filament current on one sub grid inside the vacuum vessel.

By using the plasma current vector I_p calculated by formula (6), the major radius R_{center} and vertical position Z_{center} of plasma current center can be predicted using the following formula.

$$R_{center} = \frac{\sum_{i=1}^n r_i I_{Pi}}{\sum_{i=1}^n I_{Pi}}; Z_{center} = \frac{\sum_{i=1}^n z_i I_{Pi}}{\sum_{i=1}^n I_{Pi}} \tag{7}$$

Here, n is the amount of the plasma sub grids, (r_i, z_i) is the position of each plasma sub grid and I_{Pi} is the plasma current on each sub grid.

Determination of the Response Matrices

According to formula (6), the response matrices need to be pre-calculated for the prediction of the plasma current

center. The response matrices are independent of the experimental diagnostic data. We can calculate the response matrices based on the physical parameters of the device.

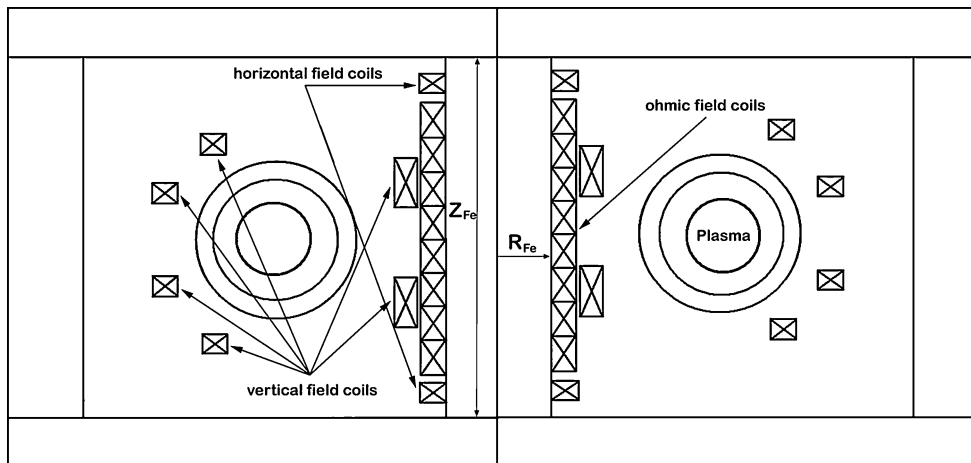
HT-7 is an iron-core tokamak. We can calculate the poloidal magnetic flux of HT-7 with a spool model for the iron core, which was developed for the TEXT-Upgrade [8]. The shape of the iron core and the geometry of the poloidal field coils in HT-7 is shown in Fig. 2. The iron core spool model is shown in Fig. 3. In the spool model, the radius R_{Fe} of the cylindrical central post is the actual radius of the iron core in HT-7. The radius R_d of the two disks on the top and bottom is chosen beyond any poloidal field coils. The distance between the top and the bottom disks, Z_{Fe} , is a free parameter. We chose the actual height of the iron core in HT-7 for Z_{Fe} . The choice is made by comparing experimental HT-7 results with our calculation based on this model.

Based on the spool model, we suppose a current I_s flowing in a coil at (R_s, Z_s) , where R_s is the radius of the coil and Z_s is the vertical distance from the mid-plane of the tokamak. The poloidal magnetic flux Ψ at (R, Z) is given by [8]

$$\begin{aligned} \Psi(R, Z) = & L_m I_s - \frac{\mu_0 \pi I_s}{Z_{Fe}} (R_s^2 + R^2) + \frac{\mu_0 \pi I_s}{Z_{Fe}} \left\{ \begin{array}{l} R^2; R_{Fe} < R < R_s \\ R_s^2; R > R_s \end{array} \right\} \\ & + \frac{4\mu_0 \pi I_s R R_s}{Z_{Fe}} \times \sum_{n=1}^{\infty} \cos \left[n \left(\frac{\pi Z}{Z_{Fe}} + \frac{\pi}{2} \right) \right] \cos \left[n \left(\frac{\pi Z_s}{Z_{Fe}} + \frac{\pi}{2} \right) \right] \\ & \times \left[\frac{I_0 \left(\frac{n\pi R_{Fe}}{Z_{Fe}} \right)}{K_0 \left(\frac{n\pi R_{Fe}}{Z_{Fe}} \right)} K_1 \left(\frac{n\pi R}{Z_{Fe}} \right) K_1 \left(\frac{n\pi R_s}{Z_{Fe}} \right) \right. \\ & \left. + \left\{ \begin{array}{l} I_1 \left(\frac{n\pi R}{Z_{Fe}} \right) K_1 \left(\frac{n\pi R_s}{Z_{Fe}} \right); R_{Fe} < R < R_s \\ K_1 \left(\frac{n\pi R}{Z_{Fe}} \right) I_1 \left(\frac{n\pi R_s}{Z_{Fe}} \right); R > R_s \end{array} \right\} \right] \end{aligned} \tag{8}$$

Here, L_m is the iron core’s magnetic resistance, $I_\alpha(x)$ and $K_\alpha(x)$ are the first and second kind modified Bessel

Fig. 2 Shape of the iron core and the geometry of the poloidal field coils in HT-7



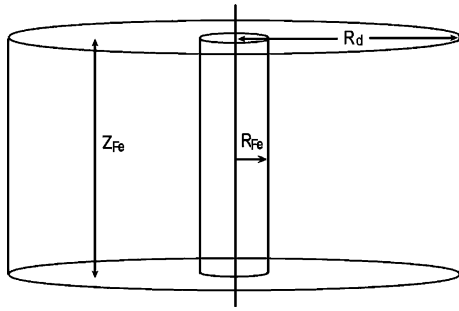


Fig. 3 Spool model of the iron core

functions. Then the magnetic field can be calculated by the formula below.

$$B_R = -\frac{1}{2\pi R} \frac{\partial \Psi}{\partial Z} = G_{rs} I_s; B_Z = \frac{1}{2\pi R} \frac{\partial \Psi}{\partial R} = G_{zs} I_s \quad (9)$$

Here, G_{rs} are G_{zs} are the response matrices which are used to calculate the magnetic field in two directions respectively, the radial direction and the vertical direction. We can derive the formulas of response matrices by using (8–9).

$$G_{rs}(R, Z) = \frac{2n\mu_0\pi R_s}{Z_{Fe}^2} \times \sum_{n=1}^{\infty} \sin \left[n \left(\frac{\pi Z}{Z_{Fe}} + \frac{\pi}{2} \right) \right] \cos \left[n \left(\frac{\pi Z_s}{Z_{Fe}} + \frac{\pi}{2} \right) \right] \times \left[\frac{I_0 \left(\frac{n\pi R_{Fe}}{Z_{Fe}} \right)}{K_0 \left(\frac{n\pi R_{Fe}}{Z_{Fe}} \right)} K_1 \left(\frac{n\pi R}{Z_{Fe}} \right) K_1 \left(\frac{n\pi R_s}{Z_{Fe}} \right) + \left\{ \begin{array}{l} I_1 \left(\frac{n\pi R}{Z_{Fe}} \right) K_1 \left(\frac{n\pi R_s}{Z_{Fe}} \right); R_{Fe} < R < R_s \\ K_1 \left(\frac{n\pi R}{Z_{Fe}} \right) I_1 \left(\frac{n\pi R_s}{Z_{Fe}} \right); R > R_s \end{array} \right\} \right] \quad (10)$$

$$G_{zs}(R, Z) = - \left\{ \begin{array}{l} 0; R_{Fe} < R < R_s \\ \frac{\mu_0}{Z_{Fe}}; R > R_s \end{array} \right\} + \frac{2\mu_0 R_s}{R Z_{Fe}} \times \sum_{n=1}^{\infty} \cos \left[n \left(\frac{\pi Z}{Z_{Fe}} + \frac{\pi}{2} \right) \right] \cos \left[n \left(\frac{\pi Z_s}{Z_{Fe}} + \frac{\pi}{2} \right) \right] \times \left[\frac{I_0 \left(\frac{n\pi R_{Fe}}{Z_{Fe}} \right)}{K_0 \left(\frac{n\pi R_{Fe}}{Z_{Fe}} \right)} K_1 \left(\frac{n\pi R}{Z_{Fe}} \right) K_1 \left(\frac{n\pi R_s}{Z_{Fe}} \right) + \left\{ \begin{array}{l} I_1 \left(\frac{n\pi R}{Z_{Fe}} \right) K_1 \left(\frac{n\pi R_s}{Z_{Fe}} \right); R_{Fe} < R < R_s \\ K_1 \left(\frac{n\pi R}{Z_{Fe}} \right) I_1 \left(\frac{n\pi R_s}{Z_{Fe}} \right); R > R_s \end{array} \right\} \right]$$

$$+ \frac{2\mu_0 R_s}{Z_{Fe}} \times \sum_{n=1}^{\infty} \cos \left[n \left(\frac{\pi Z}{Z_{Fe}} + \frac{\pi}{2} \right) \right] \cos \left[n \left(\frac{\pi Z_s}{Z_{Fe}} + \frac{\pi}{2} \right) \right] \times \left[\frac{n\pi I_0 \left(\frac{n\pi R_{Fe}}{Z_{Fe}} \right)}{Z_{Fe} K_0 \left(\frac{n\pi R_{Fe}}{Z_{Fe}} \right)} K_1' \left(\frac{n\pi R}{Z_{Fe}} \right) K_1 \left(\frac{n\pi R_s}{Z_{Fe}} \right) + \left\{ \begin{array}{l} \frac{n\pi}{Z_{Fe}} I_1' \left(\frac{n\pi R}{Z_{Fe}} \right) K_1 \left(\frac{n\pi R_s}{Z_{Fe}} \right); R_{Fe} < R < R_s \\ \frac{n\pi}{Z_{Fe}} K_1' \left(\frac{n\pi R}{Z_{Fe}} \right) I_1 \left(\frac{n\pi R_s}{Z_{Fe}} \right); R > R_s \end{array} \right\} \right] \quad (11)$$

Considering the response matrices G_{ts} , G_{ns} shown in the formulas (5–6) and G_{rs} , G_{zs} calculated by formulas (10–11) are in different coordinate systems, we should transform the response matrices from Cartesian coordinate system to polar coordinate system using formula below.

$$G_t = G_R \cos \theta + G_Z \sin \theta; G_n = G_R \cos(\theta - 90^\circ) + G_Z \sin(\theta - 90^\circ) \quad (12)$$

Here, θ is the tangential angle of the probes, which are distributed counterclockwise along the poloidal circle on HT-7.

In the next section, we will evaluate and validate the response matrices, which are calculated by using formulas (10–12). Using the available response matrices and measured magnetic signals on HT-7, we will evaluate the plasma current center position by using formulas (6–7) for several typical discharges and analyze the comparison between the predicted values and the experimental measurement that mentioned in the Sect. 2.

Results and Discussions

Simulation of the Measurement of Plasma Displacement by Single-Turn Flux Loops

As described above, the measurement of plasma displacement by using single-turn flux loops has limitations. On the one hand, the formula (3–4) is applicable under the assumption that $\Delta r < a_p < a_0 < R_0$. It means the plasma center should inside of a small bounded neighborhood of the tokamak center. On the other hand, we cannot determine the Shafranov shift during discharge. To be convenient, we use the measured value shown in the left side of formulas (4) to represent the horizontal displacement of plasma approximately.

To evaluate the influence of the assumption in this technique, we simulate the condition that dissatisfied the assumption in EAST using EFIT code [9, 10]. The results are presented in Fig. 4. In EAST, the major radius is

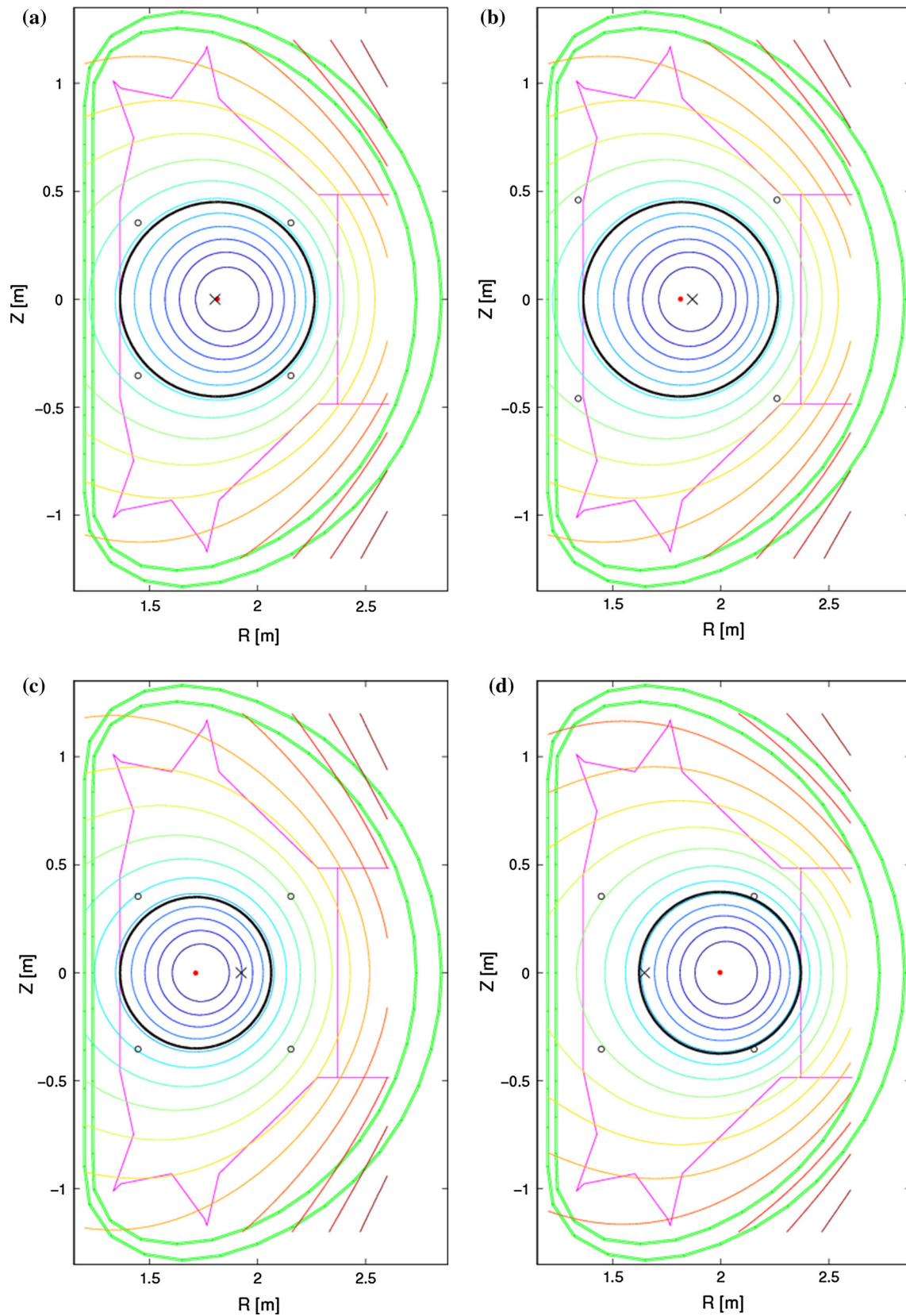


Fig. 4 The simulation of studying the influence of the assumption in the measurement of plasma displacement with the *circles* indicating the location of the flux loops. (a) and (b) The applicability of this

technique under the assumption. (c) and (d) The prediction of this technique when the assumption is dissatisfied. The calculation results by using this technique (*black x-mark*) and the exact value (*red point*)

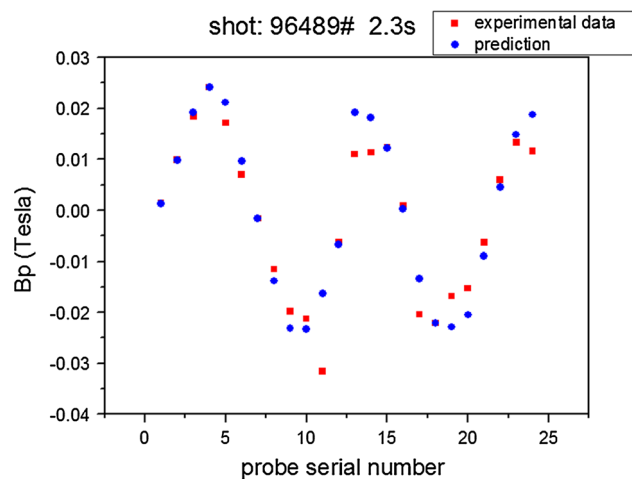


Fig. 5 Comparison of the measured magnetic signals (*square points used*) with the predicted values (*circle points used*) for a HT-7 testing shot 96489# in 2.3 s

1.80 m and the minor radius is about 0.4 m. The plasma horizontal displacement is 1.81 m in Fig. 4a and b, 1.71 m in Fig. 4c and 2.00 m in Fig. 4d. The Fig. 4a indicates the applicability of this technique under the assumption. The Fig. 4c, d shows that it failed to measure the plasma center

by using this technique when the assumption is dissatisfied. By a logical extension of this point, if the plasma center is far away from tokamak center during discharge in HT-7, the measurement of plasma displacement is inaccurate. The Fig. 4b presents that the measurement results become more accurate while the flux loops approach the outmost magnetic surface.

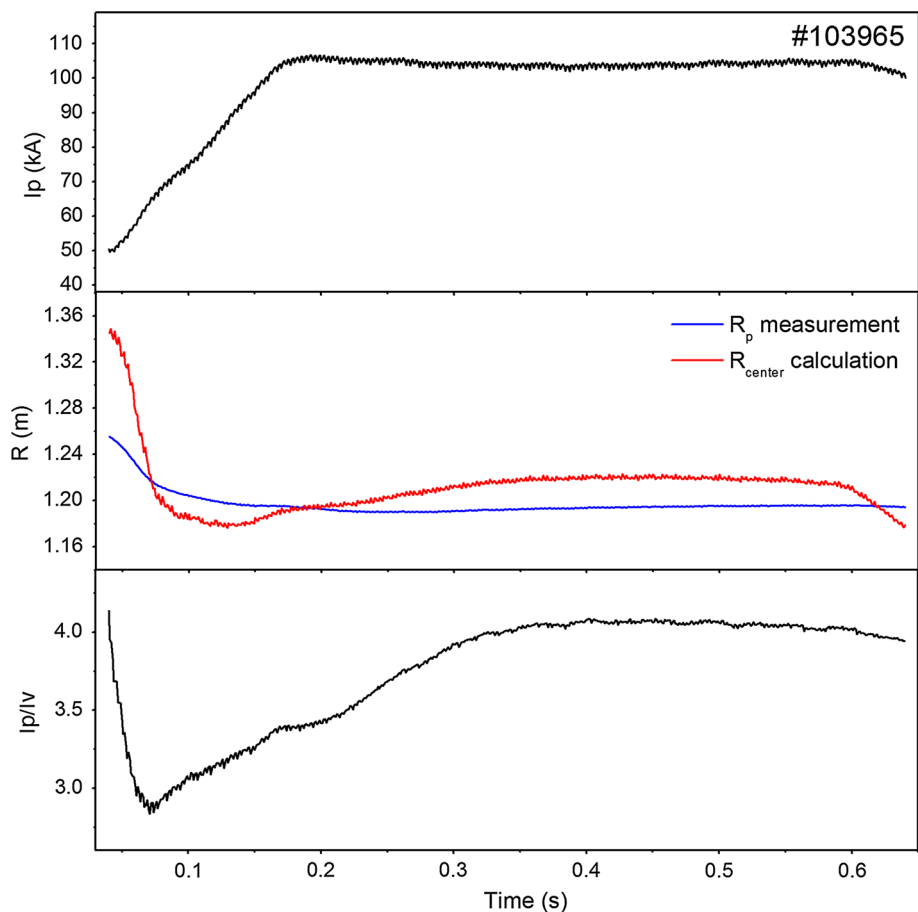
Validation of the Response Matrices

Before we predict the position of plasma current center based on the magnetic measurement, benchmark tests are performed to evaluate and validate the response matrices calculated by using formulas (10–12). We selected a testing shot #96489 without plasma, during which only the vertical field coils has power supply. We compare the measured magnetic signals with our calculation based on the formula (13).

$$B_p = G_v \cdot I_v \tag{13}$$

The comparison is shown in Fig. 5 below. Considering the measurement error of the probes, the calculated and the measured values consistent with each other perfectly and

Fig. 6 Prediction of the major radius R of plasma current center and comparison with the plasma horizontal displacement values that measured by single-turn loops for ohmic discharge #103965



the calculated response matrices are evaluated to be valid and available.

The Major Radius of the Plasma Current Center

Since the response matrices have been calculated and validated, we will evaluate the plasma current center based on the magnetic measurement, analyze the R_{center} results and the plasma horizontal displacement values R_p that measured by single-turn loops on HT-7.

In HT-7, the magnetic field induced by the ohmic field coils current is mainly confined in the iron core far away from the vacuum vessel. In this case, the vertical magnetic field in HT-7 is mostly induced by the current flowing in the vertical field coils. As shown in formula (9), the vertical magnetic field is directly proportional to the vertical field coils current. Moreover, in the large aspect-ratio approximation, the external vertical field can be derived in the form [1]:

$$B_v = -\frac{\mu_0 I_p}{4\pi R_p} \left(\ln \frac{8R_p}{a_p} + A - \frac{1}{2} \right) \quad (14)$$

Thus the horizontal displacement of plasma can be expressed as the form:

$$R_p = -\frac{\mu_0 I_p}{4\pi B_v} \left(\ln \frac{8R_p}{a_p} + A - \frac{1}{2} \right) \propto \frac{I_p}{I_v} \quad (15)$$

Here, I_p is the plasma current and I_v is the current that flows in the vertical field coils. When the plasma current maintains unchanged, with the absolute value of the vertical field coil current increasing, the strength of the vertical magnetic field enhances. As a result, the inward Lorentz force that against the plasma current strengthens. It means that the plasma current center will move toward inside of the vacuum vessel; conversely, it will move outside.

The Fig. 6 shows the result of a typical ohmic discharge #103965. The plasma horizontal displacement R_p including Shafranov shift that measured by single-turn loops directly is presented in blue line, and the red line presents the estimation of the major radius of the plasma current center R_{center} . During discharge, the plasma current and position are affected by the vertical field coils current in HT-7. According to the analysis above, shown in the formula (15), the plasma horizontal displacement should change following the ratio of plasma current and the vertical field coils current I_p/I_v , when the plasma current ramps up to the flattop after 180 ms.

Fig. 7 Prediction of the major radius R of plasma current center and comparison with the plasma horizontal displacement values that measured by single-turn loops for ohmic+LHCD discharge #104700

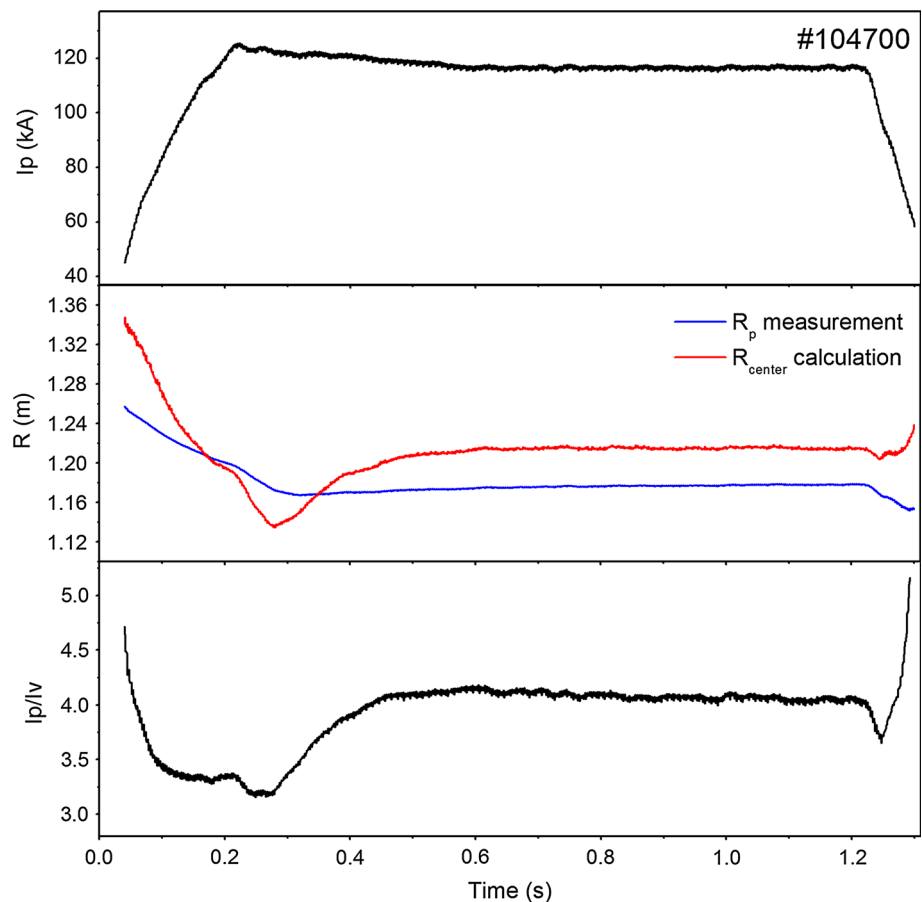
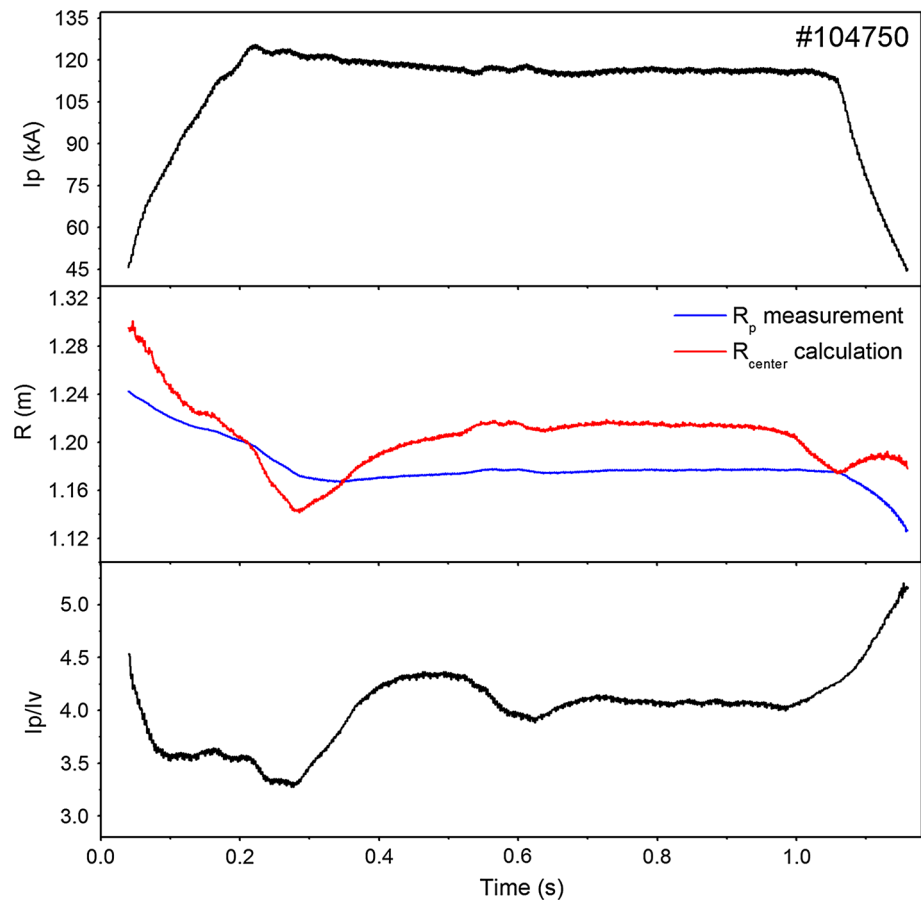


Fig. 8 Prediction of the major radius R of plasma current center and comparison with the plasma *horizontal* displacement values that measured by single-turn loops for ohmic+ICRF discharge #104750



For the ohmic shot #103965, during 180–350 ms, the ratio of plasma current and the vertical field coils current increase obviously. Following the change, the plasma should move from outside to inside toward horizontal direction, which means the horizontal displacement R_p should increase during this phase. However, the measurement by using single-turn flux loops failed to reflect the tendency. On the other hand, the major radius of the plasma current center R_{center} we estimated reflected the trend of the vertical magnetic field. After 350 ms, the plasma current center turns into the steady state as the plasma current and the vertical field coils current retain in the equilibrium state. In HT-7, the plasma current center is nearby the magnetic axis and the magnetic axis is outside the plasma outmost magnetic surface about 1–2 cm (the major radius of HT-7 is 1.22 m and the minor radius is 0.27 m). The R_{center} stays outside of the plasma horizontal displacement which is the measurement R_p plus the Shafranov shift (about 2 cm in HT-7) about 1 cm, which is also reasonable.

In addition, we select three discharges with auxiliary heating and current drive on HT-7 to verify this method. As shown in Figs. 7 and 8, the R_{center} results are consistent with the trend of the ratio I_p/I_v very well. In particular, during the current flattop phase at about 280 ms in these

three discharges, the ratio I_p/I_v reaches its bottom and then increases. The horizontal displacement R_p should reach bottom after that moment and then increases, which means the plasma reach the innermost position and then move towards outside. Unfortunately, the R_p measured by using single-turn flux loops failed to reflect the change and kept unchanged. Furthermore, as the shot #104750 shown in Fig. 8, the ratio I_p/I_v shifts significantly from 550 to 650 ms. Relatively, the R_{center} calculated based on the magnetic measurement reflect the tendency expressly. About the invalidation of measurement by single-turn loops, as simulated and analyzed in Sect. 4.1, this technique will become invalid when the assumption $\Delta r \ll a_p < a_0 \ll R_0$ is dissatisfied.

The Vertical Position Z of the Plasma Current Center

By now, we cannot get the effective experimental data of the horizontal field coils current. Its change mainly affects the trend of the vertical position of plasma current center, as the vertical field coils current to the horizontal position of the plasma current center. Here we could not discuss the calculation of vertical position of the plasma current center.

In future, we could gather the experimental data of the horizontal field coils current for further analysis.

Summary

In this study, we found out the plasma horizontal displacement value, which was measured directly by single-turn loops, had failed to reflect the change of plasma current center on HT-7, especially during the plasma breakdown phase. We did the simulation of this measurement method and analyzed the limitation of measuring the plasma displacement by using single-turn loops. In addition, we attempted to evaluate the plasma current center by using external magnetic measurement on iron-core tokamak HT-7. The calculation showed that this simplified method was validated to evaluate the horizontal position of plasma current center for the discharges on HT-7. The prediction of vertical position of the plasma current center need to be further examined. Besides, we need to modify the response matrices to improve the absolute value

accuracy of the prediction during practical discharges. Further, this simplified method could be used for the determination of plasma current center on the iron-core tokamak.

Acknowledgments This work was supported by the National Magnetic Confinement Fusion Research Program of China under Grant Nos 2012GB105000 and 2014GB103000. The authors gratefully acknowledge the contribution of the EAST&HT-7 staff.

References

1. J. Wesson, *Tokamaks* (Oxford University Press, Oxford, 1997)
2. A. Pironti, M. Walker, *IEEE Control Syst. Mag.* **25**, 30 (2005)
3. A. Beghi, A. Cenedese, *IEEE Control Syst. Mag.* **25**, 44 (2005)
4. B.J. Xiao et al., *Fusion Eng. Des.* **83**, 181 (2008)
5. Y.B. Zhu et al. in *Proceedings of the 1996 International Conference on Plasma Physics* **1** 1426 (1997)
6. V.S. Mukhovatov, V.D. Shafranov, *Nucl. Fusion* **11**, 605 (1971)
7. B. Shen et al., *Rev. Sci. Instrum.* **78**, 093501 (2007)
8. E.R. Solano et al., *Nucl. Fusion* **30**, 1107 (1990)
9. L.L. Lao et al., *Nucl. Fusion* **25**, 1611 (1985)
10. J.P. Qian et al., *Plasma Sci. Technol.* **11**, 142 (2009)